Orbital magnetic moment in Ir doped $CaMnO_3$

2009 J. Phys.: Condens. Matter 21 336001

(http://iopscience.iop.org/0953-8984/21/33/336001)

J. Phys.: Condens. Matter **21** (2009) 336001 (5pp) doi:10.1088/0953-8984/21/33/336001

Orbital magnetic moment in Ir doped $CaMnO_3$

S Mizusaki[1,5], Y Toyoda[1], T Ohnishi[1], Y Nagata[1], M Itou[2], Y Sakurai[2], Y Noro[3] and T C Ozawa[4]

[1] Department of Electrical Engineering and Electronics, Aoyama Gakuin University, Fuchinobe, Sagamihara, Kanagawa 157-8572, Japan
[2] Japan Synchrotron Radiation Research Institute (JASRI/SPring-8), Sayo, Hyogo 679-5198, Japan
[3] Kawazoe Frontier Technologies, Co. Ltd., Kuden, Sakae, Yokohama, Kanagawa 931-113, Japan
[4] Nanoscale Materials Center, National Institute for Materials Science, Namiki, Tsukuba, Ibaraki 305-0044, Japan

E-mail: smizusaki@ee.aoyama.ac.jp

Received 3 April 2009, in final form 25 June 2009
Published 24 July 2009
Online at stacks.iop.org/JPhysCM/21/336001

Abstract

The magnetism of $CaMn_{0.55}Ir_{0.45}O_3$ has been studied using the magnetic Compton scattering technique. The analysis of the magnetic Compton profile shows that the spin moments of Mn and Ir form an antiparallel configuration, establishing ferrimagnetism. Moreover, the experimental results indicate the existence of an orbital moment 0.2 μ_B/f.u.. The possible model for these results has been discussed under the framework of the localized electron model by taking account of the electronic states of the Ir^{4+} ion.

1. Introduction

Knowledge of the orbital magnetic moment permits us to understand the relationship between the spin–orbit coupling and magnetic properties of the substances. The behavior of 4d or 5d transition metal elements in oxide systems has attracted significant attention [1] due to the strong spin–orbital coupling caused by their larger orbital extent as compared with that of 3d metal ions. Already, many interesting phenomena have been observed for iridium oxide systems [1–5, 8], and the theoretical calculation for the electronic structure of Ir oxides has been performed [6, 7]. The Ir oxide system is very interesting to study for the magnetic contribution of 5d electrons because of the remains of the orbital moment on the Ir ion.

In the previous work on the $CaMn_{1-x}Ir_xO_3$ ($0 \leqslant x \leqslant 0.6$) system [9], we reported that ferromagnetism was induced in the antiferromagnetic Mott insulator $CaMnO_3$ by Ir doping (see figure 1), with the crystallography homogeneous in the range of $0 \leqslant x \leqslant 0.6$. In this system, antiferromagnetism is observed for samples with $x = 0.05$–0.2, however, ferromagnetism appears at about $x = 0.3$ and persists up to $x = 0.6$. As shown in figure 1, in the transition from antiferromagnetism to ferromagnetism, T_N is superseded by T_C without passing 0 K. The previous works leaves the issue of the interaction between Mn and Ir ions and of the relation between the magnetization and spin moment of the $CaMn_{1-x}Ir_xO_3$ system.

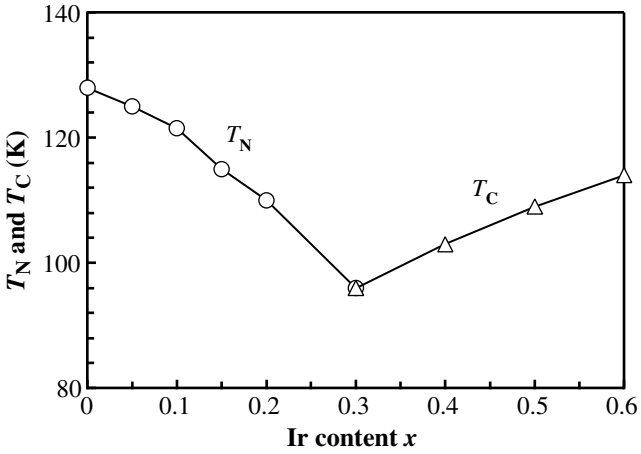

Figure 1. Ir-content dependence of the Néel temperature T_N and the Curie temperature T_C of $CaMn_{1-x}Ir_xO_3$ ($0 \leqslant x \leqslant 0.6$) [9].

[5] Author to whom any correspondence should be addressed.

Therefore, we investigate the magnetic ground states of the Ir ion in $CaMn_{0.55}Ir_{0.45}O_3$ using the magnetic Compton scattering (MCS) experiment.

MCS is a powerful tool to study the magnetic structure of materials [10–19] because the MCS samples only the spin moment and provides the magnetic Compton profile (MCP), $J_{\mathrm{mag}}(p_z)$. The MCS experiment has yielded the spin moment of the $CaRu_{1-x}Mn_xO_3$ system [16–18], $CaRu_{0.85}Fe_{0.15}O_3$ [13, 14], and $SmFe_2$ [19]. Therefore, the magnetic Compton scattering experiment is a suitable tool to obtain information on the magnetic ground state of $CaMn_{0.55}Ir_{0.45}O_3$.

2. Experiment

Polycrystalline $CaMn_{0.55}Ir_{0.45}O_3$ was prepared by the usual solid-state reaction method, which is described in detail in a previous paper [9]. The crystal structure was characterized by x-ray powder diffraction using Cu Kα radiation and subsequent refinement by the Rietveld method. The XRD profiles and the result of the refinement showed that the sample was single phase and had a $GdFeO_3$-type orthorhombic perovskite structure of space group $Pbnm$.

The MCS experiment was performed using the beamline BL08W of SPring-8 after cooling the specimen down to 10 K under an applied field of 2.5 T. The energy spectrum of the scattered flux was measured using a 10-element Ge detector at a mean scattering angle of 175° through the Sn filter, which absorbed the fluorescent x-ray flux from Ir. The overall momentum resolution was 0.57 atomic units (a.u.), where 1 a.u. of momentum is defined as 1.99×10^{-24} kg m s^{-1}. The details of the experiment are described in [10]. The total spin moment was assigned by comparing the MCP with that obtained for polycrystalline Fe. The total number of counts for each detector was 7×10^6 for 100 h in the charge Compton profiles. The usual data correction procedures were applied to the results, and, after the symmetry of the profiles was checked with respect to the zero momentum, the MCP's were folded at zero momentum to increase the effective statistical precision of the data. The amplitude of the MCP spectra, $J_{\mathrm{mag}}(p_z)$, was calibrated, using the data obtained for Fe under the same experimental conditions, to correct for the partial circular polarization of the incident beam and other geometrical factors.

The magnetic properties were characterized using a SQUID magnetometer at temperatures between 5 and 350 K under an applied magnetic field up to 5.5 T.

3. Results and discussion

3.1. Magnetic properties

The temperature dependence of magnetization, J, of $CaMn_{0.55}Ir_{0.45}O_3$ is shown in figure 2. FC and ZFC indicate the results obtained with and without applying magnetic fields of 0.1 and 2.5 T. Ferromagnetic behavior, with T_C of 110 K, was clearly observed. The values of the magnetization J were 0.10 μ_B/f.u. for ZFC cooling conditions and 0.30 μ_B/f.u. for FC cooling conditions at 10 K under 2.5 T. The $M(T)$ under FC cooling condition shows the typical characteristic of a ferromagnet with a large thermal hysteresis.

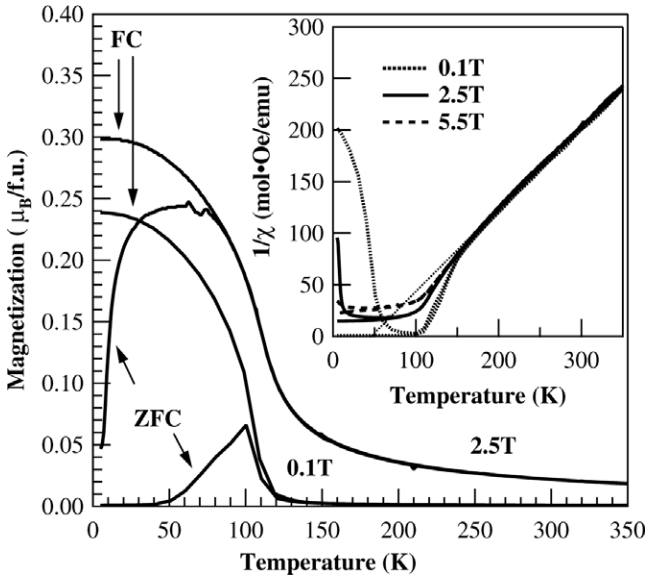

Figure 2. Temperature dependence dc magnetization for $CaMn_{0.55}Ir_{0.45}O_3$ measured under ZFC and FC ($H = 2.5$ T) cooling conditions.

In figure 2, the ZFC–$M(T)$ curve starts from very small value and increases with increasing temperature; however, the magnetization decreases after showing a maximum close to the Curie temperature T_C. On the other hand, the FC–$M(T)$ curve shows a typical ferromagnetic behavior. The FC and ZFC curves coincide at higher temperatures. The irreversible temperature, at which FC and ZFC curves split, decreases as the applied field increases and is 100 K, 70 K, and 10 K at 0.1 T, 2.5 T, and 5.5 T, respectively. In general, polycrystalline ferromagnetic oxides with relatively large magnetic anisotropy show this type of thermal hysteresis. Therefore, the large thermal hysteresis in the $M(T)$ curve suggests the existence of a large magnetocrystalline anisotropy.

The inset of figure 2 shows the temperature dependence of the reciprocal susceptibility, $\chi^{-1}(T)$, under fields of 0.1, 2.5 and 5.5 T. The Curie–Weiss fit for $\chi^{-1}(T)$ yields a Weiss temperature $\theta_W \sim +50$ K and an effective moment $\mu_{\mathrm{eff}} = 3.17\ \mu_B$/f.u.. Within the framework of the localized electron magnetism, the positive θ_W indicates the existence of a ferromagnetic interaction in $CaMn_{0.55}Ir_{0.45}O_3$.

Figure 3 shows the magnetic hysteresis curves measured under ZFC and FC conditions up to ±5.5 T. The sample has a large coercive force, H_c, of about 4 T and no saturation is observed up to 5.5 T. Moreover, the $M(H)$ curve of FC condition shifts in the positive direction of the magnetization axis. Similar phenomena have been observed for $Sr_3Ir_2O_7$ [20], Co_2VO_4 [21], $LuVO_3$ [22], and $LaFeO_3$ [23] and explained by a model which assumes the coexistence of a hard magnetic component with very large coercive force and a component with a symmetrical hysteresis loop. For example, in the $LaFeO_3$ case, the hysteresis loop was explained by a two-phase magnetic system containing α-Fe_2O_3 and $LaFeO_3$, where the symmetrical loop of α-Fe_2O_3 is superimposed on a hard

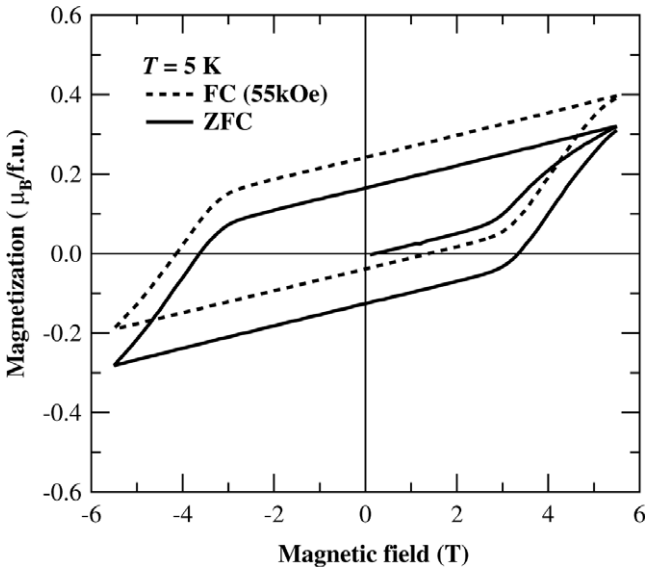

Figure 3. The isothermal magnetization curve $M(H)$ for $CaMn_{0.55}Ir_{0.45}O_3$ as a function of magnetic field measured under ZFC and FC ($H = 5.5$ T) conditions.

magnetic component of $LaFeO_3$. Our case seems different from that case because our sample is characterized as a single phase crystallographically homogeneous system, as mentioned in the previous paper [9]. In the case of vanadium oxide [22], a similar phenomenon is considered to be associated with the unquenched orbital magnetic moment of the V^{3+} ($3d^2$), and the spin–orbit coupling aligns the spin moment and orbital moment along the applied magnetic field direction. If a large orbital magnetic moment exists, this model is suitable to explain the results for $CaMn_{0.55}Ir_{0.45}O_3$.

3.2. Magnetic Compton scattering

The MCS experiment provided the absolute value of the spin moment under the ZFC cooling and FC cooling process. The assigned magnetic moments are listed in table 1. The absolute value of μ_S at 10 K under 2.5 T was 0.088 $\mu_B \pm 0.005$ μ_B/f.u. for both cooling conditions. The fact is that the spin moment is small for $CaMn_{0.55}Ir_{0.45}O_3$. It was found that the orbital moment for $CaMn_{0.55}Ir_{0.45}O_3$ was 0.21 μ_B/f.u. for FC conditions and ~ 0 μ_B/f.u. for ZFC conditions, respectively. Orbital magnetic moments, μ_L, were calculated from the μ_S and the total bulk moment (magnetization; J) by the magnetization measurement. This result indicates that the spin moment would be canceled out. It is very interesting that the spin moment is very tiny and to consider whether this orbital moment originates from the Mn or Ir ion.

The experimental magnetic Compton profile (MCP) is shown in figure 4(a) to reveal the component of spin moment of $CaMn_{0.55}Ir_{0.45}O_3$. The distribution of experimental MCP, J_{mag}, shows the Mn moment was induced along the applied magnetic field direction, and it was a dominant component of the spin moment rather than the Ir moment. The reason is that the experimental MCP, J_{mag}, is distributed in the momentum range between -6 and $+6$ a.u. with positive values. In general,

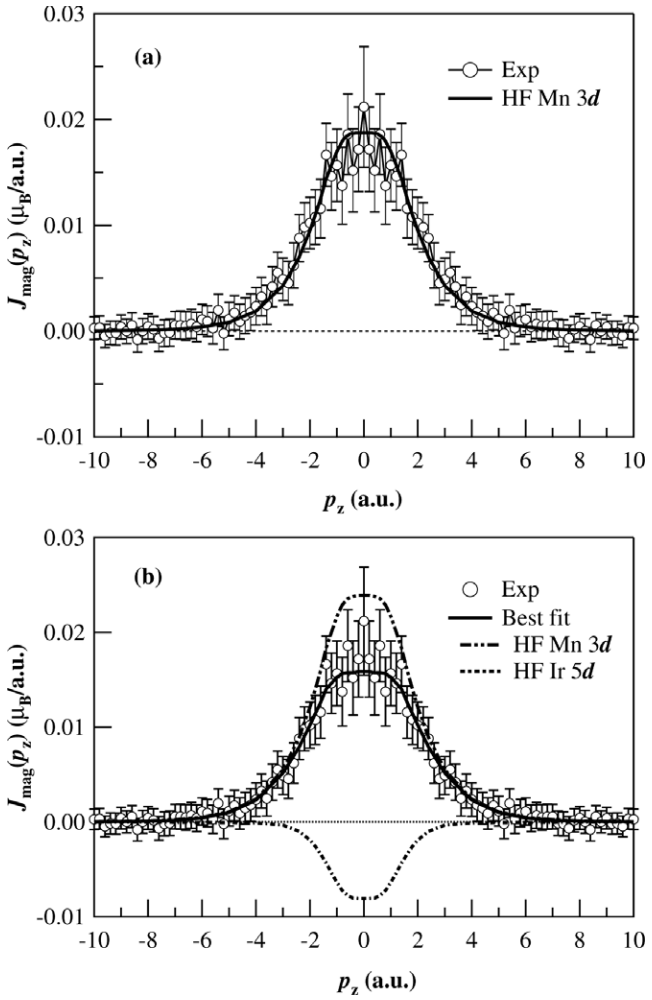

Figure 4. (a) The experimental magnetic Compton profile (MCP) at 10 K under 2.5 T together with the calculated Mn (3d electron) profile, whose area was calibrated to the total spin moment. (b) The experimental MCP are decomposed into RHF Mn 3d atomic and Ir 5d atomic profiles.

Table 1. Experimental results of magnetic moment of $CaMn_{0.55}Ir_{0.45}O_3$ at 10 K. The errors for the estimated values are ± 0.005 μ_B/f.u. for the spin moment and orbital moment, respectively.

	$S(\mu_B)$	$J(\mu_B)$	$L(\mu_B)$
FC	0.088	0.300	0.212
ZFC	0.088	0.110	0.022

the Compton profile of the 3d, 4d or 5d electron orbital has a characteristic distribution; for example, $J_{mag}(p_z)$ of 3d, 4d or 5d electrons distributes in the range of $|p_z| < 6$ a.u. or $|p_z| < 4$ a.u., respectively. Moreover, the agreement of the calculated RHF profile of the Mn 3d electron [25] to within the statistical error of the experimental results suggested that the Mn moment was the major component on the experimental MCP. Consequently, the MCS experiment suggested that $CaMn_{0.55}Ir_{0.45}O_3$ has an orbital moment, $\mu_L = 0.21$ μ_B/f.u. and a spin moment, $\mu_S \sim 0.01$ μ_B/f.u.

The results of the MCS experiment for $CaMn_{0.55}Ir_{0.45}O_3$ shows a competing result for the existence of an orbital

moment, $\mu_L = 0.21\ \mu_B$/f.u., and a tiny spin moment, $\mu_S \sim 0.01\ \mu_B$/f.u.. The induction of the orbital moment would originate from the Ir ions, because the μ_L of the Mn ion is generally almost quenched in the crystal. Therefore, the competition for the MCS experiment would be indirect evidence of the induction of the magnetic moment on Ir ion.

Figure 4(b) shows that the fit to the calculated profile, assuming the contributions of Mn 3d and Ir 5d electrons, agrees to the experimental MCP within the statistical error. The accordance indicates that the tiny spin moments would be consisted as a positive component on Mn, μ_S^{Mn}, and as a negative component on Ir, μ_S^{Ir}, which would couple antiferromagnetically. Therefore, the ferrimagnetism would be described by the antiferromagnetic coupling from the superexchange interaction between the Mn ($3d^3$) ion with μ_S^{Mn} and the Ir ($5d^5$) ion with μ_S^{Ir} and μ_L^{Ir} via the O^{2-} ion.

As mentioned above, the origin of the orbital moment: μ_L on the Ir ions should be attributed to the Ir^{4+} ($5d^5$) ions. In general, the μ_L of 3d ions is quenched by the crystal-field effect, however, the μ_L of 5d ions often remains due to their electron orbital having a larger spatial extent than that of the 3d electrons [24, 26]. The Ir^{4+} ($5d^5$) ion is considered to prefer a low spin state in $CaMn_{0.55}Ir_{0.45}O_3$, and the μ_L of Ir^{4+} originates from the twofold degeneracy of the d_{xz} and d_{yz} orbitals, which accommodate one hole [20]. The strong spin–orbit coupling in the 5d transition metal ions most likely stabilizes a certain complex orbital order with an unquenched orbital magnetic moment [26]. The very hard magnetic component in $CaMn_{0.55}Ir_{0.45}O_3$ is considered to be induced from the orbital component of Ir^{4+} ion. Consequently, the discussion of MCS results indicates that the magnetism of the $CaMn_{0.55}Ir_{0.45}O_3$ domain would be established by the combination between an orbital moment, μ_L^{Ir}, and the ferrimagnetic spin moment originating from the coupling between the positive μ_S^{Mn} and the negative μ_S^{Ir}.

Here, a mechanism for the origin of ferromagnetism in $CaMn_{0.55}Ir_{0.45}O_3$ will be proposed based on the experimental results of MCS and magnetization measurements. When Ir ions are replaced by Mn ions for $CaMnO_3$, a ferrimagnetic domain would be formed by the induction of the antiferromagnetic superexchange interaction between μ_S^{Ir} and μ_S^{Mn}. Then, the strong spin–orbit coupling (SOC) for the Ir ion between μ_L^{Ir} and μ_S^{Ir} would generate the orbital moment of the Ir ion along the parallel direction to the μ_S^{Mn} direction. Additionally, the SOC also induces a huge single-ion anisotropy in the IrO_6 octahedron and generates a hard magnetic component. Therefore, a huge magnetic anisotropy may be shown in the ferrimagnetic domains. The hard component of the hysteresis loop (shown in figure 3) seems to originate from the orientation of the IrO_6 octahedron in a magnetic field.

Ferrimagnetic ground states of $CaMn_{0.55}Ir_{0.45}O_3$ from the MCS experiment compete with the ferromagnetic ground states as suggested by the positive Weiss temperature, θ_W, from magnetic properties measurements shown in figure 2. The interpretation of the discrepancy is that the dominant contribution of the ferromagnetic Mn^{3+}–Mn^{4+} pairs of $CaMn_{0.55}Ir_{0.45}O_3$ would be larger than that of the antiferromagnetic pairs for Mn^{4+}–Mn^{4+} pairs and Mn^{4+}–Ir^{4+} pairs. The fraction of ferromagnetic Mn–Mn pairs would be larger than that of antiferromagnetic pairs. A similar case was shown in the $CaRu_{1-x}Mn_xRuO_3$ system [27]. This interpretation indicates that the ferromagnetic Mn–Mn pairs, antiferromagnetic Ir–Mn pairs, and antiferromagnetic Mn–Mn pairs can coexist in the system.

The difference μ_L^{Ir} was shown in the FC and ZFC cooling condition in figure 3, as listed in table 1. The discrepancy would suggest the mechanism of the magnetization process of the Ir–Mn pair ferrimagnetic domain. This domain would have a large magnetocrystalline anisotropy (see figure 3) originating from the Ir^{4+} ($5d^5$) ion because it has a stronger SOC than that of the 3d or 4d elements. Then, the large SOC will give rise to a huge magnetic anisotropy [26]. In figure 2, under the ZFC cooling condition, the spontaneous moments in each ferrimagnetic domains freeze by keeping their random orientation and almost compensate each other. As a result, the μ_L^{Ir} and net moment becomes very small. In contrast, under the FC cooling condition, the spontaneous moments in the ferrimagnetic domains align to the direction of the applied magnetic field. Therefore a μ_L^{Ir} is observed and will be dependent on the strength of applied magnetic field. In addition, the results presented strongly suggest that the Ir^{4+} ion has a magnetic moment and forms a magnetic order, which is against the prediction of the paramagnetism for *Pbnm* $CaIrO_3$ [6]. These experimental results indicate that $CaMn_{0.55}Ir_{0.45}O_3$ is an orbital ferromagnet under FC conditions.

4. Conclusion

The magnetic Compton scattering experiment for $CaMn_{0.55}Ir_{0.45}O_3$ shows the existence of an orbital magnetic moment of 0.21 μ_B/f.u. The possible origin of the orbital moment was discussed by taking account of the electronic states of the Ir ion under the framework of the localized electron model.

Acknowledgments

The magnetic Compton scattering experiment was performed with the approval of JASRI (J05A08W0–0513N, and 2007B1410). We thank Dr T Muranaka of Akimitsu lab at Aoyama Gakuin University for his help in using their 5.5 T SQUID system and also for stimulating discussions. The work conducted at Aoyama Gakuin University was supported by The Private School High-tech Research Center Program of the MEXT, Japan, 2002-2006.

References

[1] Brooks M L, Blundell S J, Lancaster T, Hayes W, Pratt F L, Frampton P P C and Battle P D 2005 *Phys. Rev.* B **71** 220411(R)

[2] Cava R J, Batlogg B, Kiyono K, Takagi H, Krajewski J J, Peck W F Jr, Rupp L W Jr and Chen C H 1994 *Phys. Rev.* B **49** 11890

[3] Cosio-Castaneda C, Tavizon G, Baeza A, de la Mora P and Escudero R 2007 *J. Phys.: Condens. Matter* **19** 446210

[4] Shimura T, Inaguma Y, Nakamura T and Itoh M 1995 *Phys. Rev.* B **52** 9143
[5] Okamoto Y, Nohara M, Aruga-Katori H and Takagi H 2007 *Phys. Rev. Lett.* **99** 137207
[6] Tsuchiya T and Tsuchiya J 2007 *Phys. Rev.* B **76** 144119
[7] Maiti K 2006 *Phys. Rev.* B **73** 115119
[8] Cao G, Durairaj V, Chikara S, Delong L E, Parkin S and Schlottmann P 2007 *Phys. Rev.* B **76** 100402(R)
[9] Mizusaki S, Sato J, Taniguchi T, Nagata Y, Lai S H, Lan M D, Ozawa T C, Noro Y and Samata H 2008 *J. Phys.: Condens. Matter* **20** 235242
[10] Cooper M J, Mijnarends P E, Shiotani N, Sakai N and Bansil A 2004 *X-Ray Compton Scattering* (Oxford: Oxford University Press)
[11] Sakai N 1998 *J. Synchrotron Radiat.* **5** 937
[12] Hiraoka N, Itou M, Deb A, Sakurai Y, Kakutani Y, Koizumi A, Sakai N, Uzuhara S, Miyaki S, Koizumi H, Makoshi K, Kikugawa N and Maeno Y 2004 *Phys. Rev.* B **70** 054420
[13] Mizusaki S, Hiraoka N, Nagao T, Itou M, Sakurai Y, Taniguchi T, Okada N, Nagata Y, Ozawa T C and Noro Y 2006 *Phys. Rev.* B **74** 052401
[14] Mizusaki S, Taniguchi T, Okada N, Nagata Y, Hiraoka N, Nagao T, Itou M, Sakurai Y, Ozawa T C and Noro Y 2006 *J. Appl. Phys.* **99** 08F703
[15] Taylor J W, Duffy J A, Bebb A M, McCarthy J E, Lees M R, Cooper M J and Timms D N 2002 *Phys. Rev.* B **65** 224408
[16] Mizusaki S, Taniguchi T, Okada N, Nagata Y, Hiraoka N, Itou M, Sakurai Y, Ozawa T C, Noro Y and Samata H 2009 *J. Phys.: Condens. Matter* **21** 276003
[17] Mizusaki S, Taniguchi T, Okada N, Nagata Y, Itou M, Sakurai Y, Ozawa T C, Noro Y and Samata H 2008 *J. Appl. Phys.* **103** 07C910
[18] Taniguchi T, Mizusaki S, Okada N, Nagata Y, Mori K, Wuernisha T, Kamiyama T, Hiraoka N, Itou M, Sakurai Y, Ozawa T C, Noro Y and Samata H 2007 *Phys. Rev.* B **75** 024414
[19] Mizusaki S, Kawamura N, Taniguchi T, Itou M, Samata H, Noro Y, Sakurai Y and Nagata Y 2007 *J. Magn. Magn. Mater.* **310** 1635 Part 2
[20] Cao G, Xin Y, Alexander C S, Crow J E, Schlottmann P, Crawford M K, Harlow R L and Marshall W 2002 *Phys. Rev.* B **66** 214412
[21] Menyuk N, Dwight K and Wickham D G 1960 *Phys. Rev. Lett.* **4** 119
[22] Nguyen H C and Goodenough J B 1995 *Phys. Rev.* B **52** 324
[23] Watanabe H 1959 *J. Phys. Soc. Japan* **14** 511
[24] Singh R S, Medicherla V R R, Maiti K and Sampathkumaran E V 2008 *Phys. Rev.* B **77** 201102
[25] Biggs F, Mendelsohn L B and Mann J B 1975 *Atomic Data and Nuclear Data Table* vol 16 (New York: Academic) p 201
[26] Ohgushi K, Gotou H, Yagi T, Kiuchi Y, Sakai F and Ueda Y 2006 *Phys. Rev.* B **74** 241104(R)
[27] Taniguchi T, Mizusaki S, Okada N, Nagata Y, Lai S H, Lan M D, Hiraoka N, Itou M, Sakurai Y, Ozawa T C, Noro Y and Samata H 2008 *Phys. Rev.* B **77** 014406